Diastereoselective Control of Bacteriochlorophyll *e* Aggregation. 3^1-S-BChl *e* Is Essential for the Formation of Chlorosome-Like Aggregates

Dorte B. Steensgaard, Hainer Wackerbarth, Peter Hildebrandt, and Alfred R. Holzwarth*

Max-Planck-Institut für Strahlenchemie, Stiftstrasse 34-36, D-45470 Mülheim an der Ruhr, Germany

Received: April 6, 2000; In Final Form: July 20, 2000

We have investigated supramolecular bacteriochlorophyll (BChl) *e* aggregates in four different solvent systems. Aggregates of HPLC-purified BChl *e* species, 3^1-R-8-ethyl-12-ethyl BChl *e*, 3^1-R-8-propyl-12 ethyl BChl *e*, 3^1-S-8-propyl-12-ethyl BChl *e*, and 3^1-S-8-isobutyl-12-ethyl BChl *e*, in cyclohexane, *n*-hexane, H_2O/monogalactosyldiglyceride, or H_2O/lecithin, indicate two different aggregate structures, as judged from absorption, circular dichroism, infrared, and resonance Raman spectroscopies. Aggregates of 3^1-R-BChl (R-BChl) *e* were characterized by a 706 nm absorption band and broad C-13^1 carbonyl stretching bands at 1650−1680 cm^{-1}. In contrast, aggregates of 3^1-S-BChl (S-BChl) *e* displayed a Q_y band maximum at 717 nm and a carbonyl stretching band at 1650 cm^{-1} only. All measurements indicated that the aggregates of S-8-isobutyl-12-ethyl BChl (S[IE]BChl) *e* mimicked the supramolecular aggregates in intact chlorosomes of *Chlorobium phaeobacteroides* much better than did the R-8-ethyl-12-ethyl BChl (R[EE]BChl) *e*-type aggregate. However, when mixtures of R[EE]BChl *e* and S[IE]BChl *e* were used for aggregate formation, even small amounts of S[IE]BChl *e* were sufficient to cause the formation of chlorosome-like aggregates. We conclude that S-BChl *e* is essential for the formation of chlorosome-like aggregates. Finally, we describe a refined model for the supramolecular chlorosomal aggregate structure.

1. Introduction

Green photosynthetic bacteria possess a unique light-harvesting structure, the so-called chlorosome.[1,2] The pigment organization of the chlorosomes is fundamentally different from that of other known photosynthetic antennas, where pigments are organized into chlorophyll proteins.[3−5] In contrast, the chlorosomal bacteriochlorophylls (BChls) self-organize into supramolecular aggregates, and proteins are not essential for the structure and light-harvesting properties of this antenna.[6−11] The chlorosomes are surrounded by a lipid monolayer, and besides thousands of BChl *c*, *d*, or *e* molecules, small amounts of BChl *a* are present, probably associated with protein in the chlorosome surface.[12,13] Carotenoids and quinones are found in the chlorosomes, too, but little is known about the organization of these constituents.[14,15]

Another unique feature of chlorosomes is the presence of several homologues and diastereoisomers of BChl *c*, *d*, and *e*. They differ by the type of esterifying alcohol at C-17,[3] by the stereochemistry of the hydroxy ethyl group at C-3, and by the nature of the substituents at C-8 and C-12.[2] These substituents can be methyl, ethyl, propyl, isobutyl, or pentyl. The distribution of these homologues and diastereoisomers is significantly different in the two groups of green bacteria known, i.e., Chloroflexaceae and Chlorobiaceae. In *Chloroflexus*, BChl *c* is always found as [EM]BChl, whereas the predominant BChl species in *Chlorobium* are 8-ethyl-12-ethyl BChl ([EE]BChl) and 8-propyl-12-ethyl BChl ([PE]BChl), which typically make up 70−90% of the total BChl. The larger substituents generally occur as the S diastereoisomers. Thus, [EE]BChl and 8-isobutyl-12-ethyl BChl ([IE]BChl) are mainly found as 3^1-R-BChl (R-BChl) and 3^1-S-BChl (S-BChl) stereoisomers, respectively.[1] These different homologues and stereoisomers seem to be of physiological significance in green bacteria since it has been observed that light conditions influence the BChl homologue distribution.[16,17] When the intensity of growth light is lowered, the amount of BChl with the larger substituents at the C-8 and C-12 positions is increased, and a concomitant red-shift of the Q_y band absorption maximum ($\leq$8 nm) of the *Chlorobium* chlorosomes is noted.

In certain molecular environments BChl *c*, *d*, and *e* molecules form large aggregate structures by self-organization, characterized by a ~50 nm red-shift of the Q_y absorption band with respect to that of the monomeric species in polar organic solvents. Consequently, the pigments must be closely packed and oriented such that strong excitonic interactions result. It is believed that these aggregates form rod structures that fill the chlorosome. The rods are visible in freeze−fracture electron microscopy.[18,19] Various spectroscopic techniques have demonstrated that the building block of these aggregates involves three molecules with the central Mg of one BChl coordinated to the hydroxyl of the C-3^1 of a second BChl, which, in turn, is hydrogen-bonded to the 13^1 keto group of a third molecule.[10,20−23] The overall organization shows a long-range ordering of the BChls with Q_y transition moments aligned parallel to the long axis of the chlorosome.[24,25] A detailed structural model of a large rod-shaped aggregate similar to those in chlorosomes has been modeled for 17^3-methyl-R[MM]bacteriochlorophyllide *d*.[26] This basic model for the interaction of neighboring pigments has been confirmed recently by cross-polarization magic-angle spinning (CP-MAS) NMR spectroscopy.[9,27]

The chlorosomal aggregates can be mimicked in solvents, such as hexane,[6] CCl_4,[6] H_2O,[28] or H_2O with lipids,[29,30] or in aqueous detergent solutions.[30,31] Such models share numerous structural and spectroscopic properties with the intact chlorosome. Olson and Pedersen demonstrated that in CCl_4 [PE]-

* Corresponding author. Fax: +49 2083063951. E-mail: holzwarth@mpi-muelheim.mpg.de.

10.1021/jp0013356 CCC: $19.00
Published on Web 10/14/2000

BChl *c* forms aggregates absorbing at 710 nm whereas aggregates of [IE]BChl *c* absorb at 758 nm.[32] These authors suggested that the difference arises from the C-3[1] configuration since S-BChl is the prevalent stereoisomer of [IE]BChl while [PE]BChl mainly exists in the R-BChl form. Careful studies of the aggregation behavior of diastereoisomers of [EM]BChl *c* and the analogous Zn-[EM]bacteriochlorophyllide *d* in CH_2Cl_2 and hexane have been carried out in our group.[33−35] These studies demonstrated substantially the differences between C-3[1]-R and C-3[1]-S aggregates on the levels of dimers and higher oligomers.

In the present work, we have studied aggregates of BChl *e* diastereoisomers and homologues. Among the chlorosomal BChls, BChl *e* is unique inasmuch as it carries a formyl group in the C-7 position. Aggregates formed in various solvents systems were studied by UV−vis, circular dichroism (CD), Fourier transformed infrared (FTIR), and resonance Raman (RR) spectroscopies. The data were used to evaluate the similarities and differences between in vitro aggregates on one hand and the intact chlorosomes of *Chlorobium phaeobacteroides* on the other hand. We show that although R-BChl is the most abundant stereoisomer in these chlorosomes, S-BChl is an essential prerequisite for the formation of chlorosome-like aggregates.

2. Experimental Section

Green Bacterial Cultures. Cells for pigment extraction were cultivated as follows: *Cb. phaeobacteroides*, strain 1549 (obtained from Professor J. Ormerod, University of Oslo), was grown at 25 °C in 10 L bottles in the medium described.[36] The cultures were illuminated by weak sunlight. After 1 week, the cells (50 g total wet weight) were harvested by centrifugation at 2300*g* for 20 min and stored at −30 °C. The chlorosomes were prepared as described.[37]

Pigment Purification. Pigments were extracted from the cell pellet in acetone:methanol (7:2 v/v) by sonication. Cell debris was removed by centrifugation, and the crude pigment extract was dried in vacuo. Analytical HPLC (using a NovaPak-C18, 3.9 × 300 mm column from Waters Inc. with a flow rate of 1 mL min^{-1}) separated three major peaks of BChl e_F, of which the second showed a prominent shoulder.[38] The homologues were identified by HPLC-coupled mass spectrometry. For this purpose, the analytical HPLC procedure was carried out with a flow rate of 0.2 mL min^{-1}, and the eluents were analyzed on a Hewlett-Packard HP 5989 BMS spectrometer employing atmospheric pressure chemical ionization. Prior to preparative HPLC, the crude extract of BChls and carotenoids was fractionated on a 5 × 100 cm column with silica 60 (0.63−0.200 mm; Merck). The dry extract was dissolved in a minimal amount of CH_2Cl_2 and applied on the column. Yellow fractions containing carotenoids and quinones were eluted with pentane and green fractions containing BChl *a* and BChl *e* eluted with diethyl ether. The crude fraction of BChls was dried in vacuo. Crude BChl (200 mg) obtained from the silica column was dissolved in methanol:THF (9:1 v/v), and preparative HPLC was carried out on a Nucleosil C18 column (7 μm, 320 × 21 mm) with methanol:H_2O (95:5 v/v) at a flow rate of 4 mL min^{-1}. Three main homologues of BChl e_F were collected. The second BChl e_F fraction was rechromatographed on a Lichrosorb diol column (7 μm, 250 × 20 mm) eluted with cyclohexane:2-propanol (95:5, v/v) at a flow rate of 4 mL min^{-1}. Two BChl *e* fractions were collected. The purity of the four fractions was tested on an analytical Lichrosorb diol column (5 μm, 250 × 4 mm) eluted (1 mL min^{-1}) with the solvent described above. The identity of the BChl *e* fractions was verified by ^1H NMR and ^{13}C NMR measurements in CD_2Cl_2:CD_3OD (9:1, v/v), recorded on a DRX500 spectrometer (Bruker Analytics).

Aggregate Preparation. BChl *e* aggregates in hexane[7] were prepared by injecting 30−35 nmol of BChl *e* (unless otherwise stated) dissolved in a minimal amount of THF in 3 mL of cyclohexane or *n*-hexane. The final THF content did not exceed 0.5%. The samples were left in the dark at 4 °C for 14−15 h to complete the aggregate formation.[39] Aggregates in H_2O/lecithin[30] were prepared by mixing BChl *e* (35 nmol in methanol) with 8 μL of L-α-lecithin from fresh egg yolk (1% in methanol, w/v; Sigma) and injecting this mixture into 3 mL of 50 mM potassium phosphate buffer, pH 7.4, upon stirring. The samples were incubated at 50 °C for 2 h in the dark. Aggregates in H_2O/monogalactosyldiglyceride (MGDG)[29] were prepared by mixing 10 μL of MGDG (0.25 μg mL^{-1} in methanol) with 35 nmol of BChl *e* in methanol and injecting the mixture into 3 mL of buffer, followed by incubation at 50 °C for 30 min. The final concentration of methanol in MGDG and lecithin aggregates was 0.7%. When samples for RR measurements were prepared, a few grains of solid sodium dithionite were added to the buffer before the addition of pigment and lipids, and the sample tube was flushed with N_2 before incubation. All concentrations were determined using the extinction coefficients determined recently.[40]

Spectroscopy. Absorption spectra were recorded on a Unicam UV2 spectrophotometer with a bandwidth of 1 nm. CD spectra were measured on a Jasco J715 machine with a bandwidth of 1 nm. FT-IR spectra were recorded on a Bruker IFS66 FT-IR spectrometer using a CaF_2 cuvette with a path length of 0.2 mm. RR measurements were taken with 413 nm excitation using the experimental setup described previously.[41] The samples were placed in a 1 mL rotating cell under the exclusion of air.

3. Results

Pigment Characterization. An HPLC trace of the major BChl *e* homologues (A, B, and C) is shown in Figure 1 (lower panel, left). The peak of homologue B shows a distinct shoulder. LC-MS analysis confirmed[42] that the pigments are R[EE]BChl e_F (MW, 820) (A), [PE]BChl e_F (MW, 834 for both components) (B), and S[IE]BChl e_F (MW, 848) (C). [PE]BChl *e* was further separated by normal-phase HPLC (Figure 1, lower panel, right), resulting in the S[PE]BChl *e* and R[PE]BChl *e* diastereoisomers. The structures of these BChl *e* species are shown in Figure 1 (upper panel). The final purities of the pigments used for aggregate formation were 95% for R[EE]BChl *e* (possibly an impurity of S[EE]BChl *e*) and 98% for S[IE] BChl *e*. The R[PE]-BChl *e* and S[PE]BChl *e* fractions contained 9% and 5% of the corresponding diastereoisomer, respectively.

Absorption Spectra. Aggregation of the four BChl *e* species was performed in four different solvent systems, which are all known to promote the formation of long-wavelength absorbing aggregates. Absorption spectra in the Q_y region of aggregates of R[EE]BChl *e*, S[PE]BChl *e*, and S[IE]BChl *e* are shown in Figure 2. The spectra for the aggregates of R[PE]BChl *e* have been omitted for clarity since they are very similar to those for the aggregates of R[EE]BChl *e*. In cyclohexane, R[EE]BChl *e* shows an aggregate Q_y band at 706 nm, whereas that of S[PE]-BChl *e* is found at 699 nm. Both absorption maxima are significantly blue-shifted with respect to that of a typical chlorosome spectrum (see Figure 3). In contrast, the spectrum of S[IE]BChl *e* aggregates (maximum at 717 nm) closely resembles that of the native chlorosomes. The average widths of the Q_y band (full width at half-maximum, fwhm) for R[EE]-BChl *e* and R[PE]BChl *e* are 35 and 38 nm, respectively,

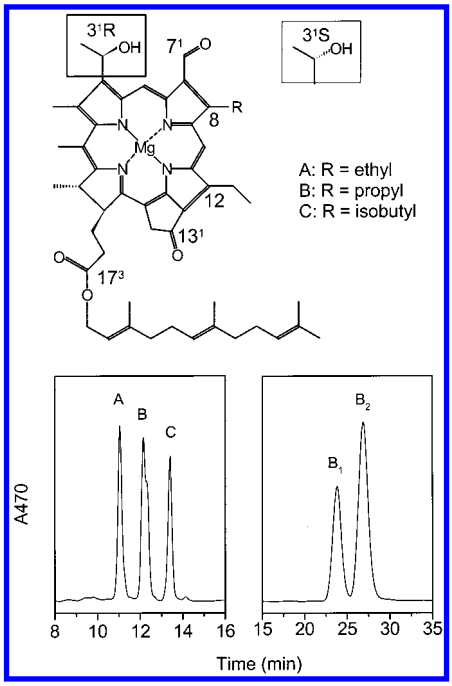

Figure 1. Structure of BChl e_F homologues and stereoisomers (top panel) and HPLC traces of the separations of these BChl *e* species (bottom panel). The substituent at C-8 is ethyl, propyl, or isobutyl. Lower left panel: the major BChl *e* homologues separated on a C18 reverse phase column; the peaks A, B, and C are assigned to R[EE]-BChl e_F, R/S[PE]BChl e_F, and S[IE]BChl e_F, respectively. Lower right panel: separation of the diastereoisomers on a normal phase column; the peaks B_1 and B_2 are assigned to S[PE]BChl e_F and R[PE]BChl e_F, respectively.

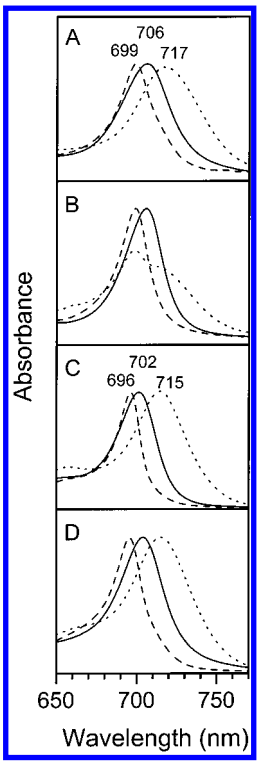

Figure 2. Absorption spectra in the Q_y region of aggregates formed from the pure BChl *e* isomers R[EE]BChl *e* (full line), S[PE]BChl *e* (dashed line), and S[IE] BChl *e* (dotted line) in (A) cyclohexane, (B) *n*-hexane, (C) H_2O/lecithin, and (D) H_2O/MGDG. The spectra were normalized to the maximum intensity for clarity.

whereas those for S[PE]BChl *e* and S[IE]BChl *e* are 26 and 49 nm, respectively. Aggregation in *n*-hexane gives similar results,

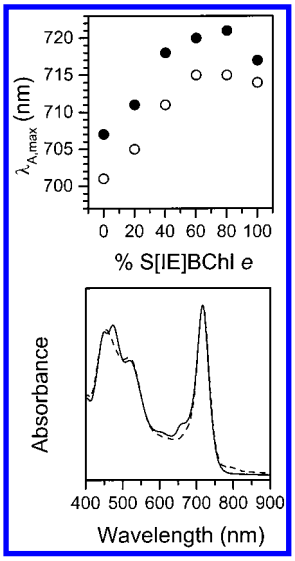

Figure 3. Aggregates of mixtures of R[EE]BChl *e* and S[IE]BChl *e*. The upper panel shows the dependence of the Q_y maximum position on the stereoisomer composition in H_2O/MGDG (open circles) and cyclohexane (filled circles). The lower panel compares chlorosomes of *Cb. phaeobacteroides* (dashed line) with aggregates of H_2O/lecithin (full line) composed of R[EE]BChl *e* and S[IE]BChl *e* (1:1).

except that the spectrum of S[IE]BChl *e* aggregates is composed of two bands at 699 and 717 nm. Immediately after the S[IE]-BChl *e* is diluted with *n*-hexane, only the 699 nm band is observed, whereas the intensity of the 717 nm band increases within many hours. Slight variations of the ratio of the 699 nm and the 717 nm components are observed between different samples. It is noted that when the 717 nm aggregates of S[IE]-BChl *e* in cyclohexane are sedimented by centrifugation and resuspended in *n*-hexane, no re-aggregation to the 699 nm form is observed within 24 h. In *n*-hexane, equilibrium between the 699 and 717 nm absorbing species is established. Since the 699 nm form of S[IE]BChl *e* in *n*-hexane has absorption properties and CD spectra (see below) similar to those of the aggregates of S[PE]BChl *e*, the 699 nm species of S[PE]BChl *e* may be a precursor of the 717 nm aggregate formed by S[IE]BChl *e*.

Aggregates in aqueous media with lipids, e.g., MGDG and lecithin, show trends similar to those of aggregates in cyclohexane. All aggregates in H_2O/lipid, however, exhibit slightly blue-shifted Q_y bands with respect to their equivalents in cyclohexane. The absorption maxima are found at 702, 696, and 715 nm for R-BChl *e*, S[PE]BChl *e*, and S[IE]BChl *e*, respectively. The bandwidths of aggregates in H_2O/MGDG and H_2O/lecithin are the same as those of aggregates in cyclohexane. In a related study on BChl *c* homologues in H_2O/MGDG, aggregates were found to absorb in the range from 724 to 745 nm, depending on the homologue species.[29] These results, however, are not directly comparable with our data since no pure diastereoisomers were used in that study.

It has previously been suggested that the extent of the red-shift of the Q_y band in chlorosome-like aggregates relative to monomer absorption depends on the size of the aggregate.[43] This would indicate that at high, supersaturated concentrations, BChl *e* in hexane tends to form more red-shifted aggregates. In our experiment, we only observe a slight broadening of the aggregate Q_y band at concentrations as high as 300 nmol mL^{-1} (data not shown). No pronounced shift is observed. Thus, our results cannot be explained by concentration effects or by differences in the solubility of the BChl *e* species. Rather, we assign the different absorption maxima to structurally different aggregates (see below).

As judged from the absorption spectra, aggregates of S[IE]-BChl *e* are much better chlorosome models than those of R-BChl *e*. This finding prompts the question of how chlorosomal BChl *e*, composed mainly of R-BChl *e*, can form aggregates in vivo that absorb at ~717 nm. To clarify this question, we let mixtures of R-BChl *e* and S-BChl *e* co-aggregate in cyclohexane and H_2O/MGDG. Figure 3 (upper panel) displays how the position of the aggregate Q_y band changes with the composition of R-BChl *e* and S-BChl *e*. Strikingly, the Q_y band position does not show a linear dependence of the mixtures of R-BChl *e* and S-BChl *e*. This shows that the aggregate Q_y band of the mixtures does not represent just a linear combination of those of the pure BChl *e* species, as would be expected for bands of noninteracting aggregates. When S[IE]BChl *e* is mixed with R[EE]BChl *e*, the aggregate absorption maximum increases from 706 nm at 0% R[EE]BChl *e* to ~720 nm in the range of 40−80% S[IE]-BChl *e*. For mixtures of R-BChl *e* and S-BChl *e* close to 1:1, the position of the aggregate Q_y band (720 nm for 60% S[IE]-BChl *e*) is even slightly higher than that for aggregates of pure S[IE]BChl *e* (717 nm). When S[PE]BChl *e* was mixed with R[EE]BChl *e*, a similar effect on the aggregate Q_y band is observed. Between 40% and 80% S-BChl *e*, the most pronounced red-shift (714 nm) is observed (data not shown). When aggregates are prepared in H_2O/lecithin, similar tendencies are found for mixtures of R-BChl *e* and S-BChl *e*. Figure 3 (lower panel) shows an example of a mixed aggregate (R[EE]BChl *e* and S[IE]BChl *e*, 1:1) in H_2O/lecithin. The spectrum is compared with that of chlorosomes from *Cb. phaeobacteroides*. In addition to the similar bandwidth (fwhm 41 ± 1 nm), the Q_y positions of both the chlorosome and the mixed aggregate are found at 717 nm. The BChl *e* composition of these chlorosomes was 32% R[EE]BChl *e*, 26% R[PE]BChl *e*, 16% S[PE]BChl *e*, and 26% S[IE]BChl *e*, respectively.

CD Spectroscopy. The CD spectra of BChl *e* aggregates in cyclohexane, *n*-hexane, and H_2O/lecithin are shown in Figure 4 (panels A, B, and C, respectively). In all solvents, the aggregates of R[EE]BChl *e* show CD spectra of type I (i.e., a positive band and a negative band at the blue and the red sides of the absorption maxima, respectively).[25] These spectra have zero crossing points at 707 and 703 nm for the aggregates in hexane and H_2O/lecithin, respectively. The crossing points are in good agreement with the positions of the absorption maxima in Figure 2. The aggregates of R[PE]BChl *e* display spectra very similar to those of R[EE]BChl *e* (data not shown). The aggregates of S[PE]BChl *e* show CD spectra of type I too, albeit less intense than those of R[EE]BChl *e* and R[PE]BChl *e*. The crossing points are again very close to the respective absorption maxima. The aggregates of S[IE]BChl *e* in cyclohexane display a very weak featureless CD signal. In *n*-hexane, a type I band with a crossing point at 698 nm is observed for S[IE]BChl *e*. As shown in Figure 2, aggregates of S[IE]BChl *e* in *n*-hexane show split aggregate Q_y bands at 699 and 718 nm. The CD spectrum of S[IE]BChl *e* aggregates in *n*-hexane, therefore, obviously originates from the 699 nm absorption species. Thus, like in cyclohexane, the 718 nm absorbing aggregate in *n*-hexane has no substantially CD intensity. H_2O/lecithin aggregates show a weak type II CD signal (i.e., a negative band and a positive band at the blue and the red sides of the absorption maximum, respectively) with a crossing point at 715 nm, corresponding to the absorption maximum of this aggregate.

The CD data on aggregates in H_2O/lecithin are in agreement with the results of Uehara et al., who found that smaller homologues (methyl and ethyl as substituents on C-8 and C-12 positions) of BChl *c* in H_2O/MGDG had CD intensities stronger than those of larger BChl *c* homologues.[29] Furthermore, these authors reported that small homologues formed aggregates with type I CD spectra, whereas those of larger BChl *c* homologues showed type II spectra. These results are in good agreement with our data. The lack of a strong CD signal in aggregates containing the 717 nm species in cyclohexane and *n*-hexane is puzzling since in chlorosome aggregates there are substantial excitonic interactions among strongly coupled pigments, leading to a large CD signal. However, two contributions are contained in the aggregate CD signal: the intrinsic CD originating from the local environment of the single BChl, and the so-called polymer-salt-induced CD that occurs in large three-dimensional polymers.[33,44] These two components may have opposite signs. It is likely that the lack of a strong CD signal for the 717 nm absorbing species in hexane is due to a cancellation of the contributions of the intrinsic and polymer-salt-induced CD

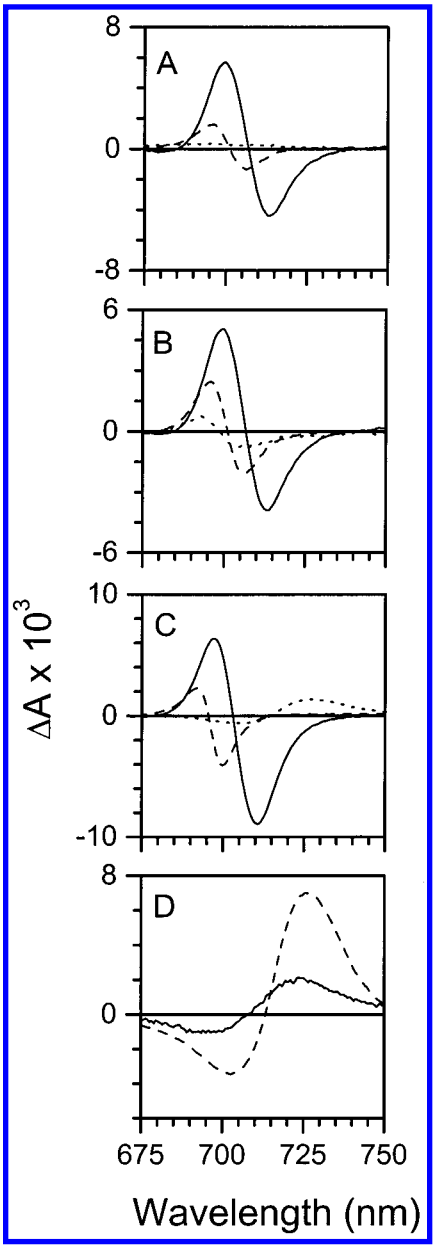

Figure 4. Circular dichroism spectra of aggregates of BChl *e* in (A) cyclohexane, (B) *n*-hexane, and (C) H_2O/lecithin. The aggregates are R[EE]BChl *e* (full line), S[PE] BChl *e* (dashed line), and S[IE]BChl *e* (dotted line). (D) The spectrum of chlorosomes of *Cb. phaeobacteroides* (dashed line) and mixed aggregates (full line) composed of R[EE]BChl *e* and S[IE]BChl *e* (1:1) in H_2O/lecithin. All spectra were normalized to an OD of 1.0 cm^{-1} in the aggregate Q_y band.

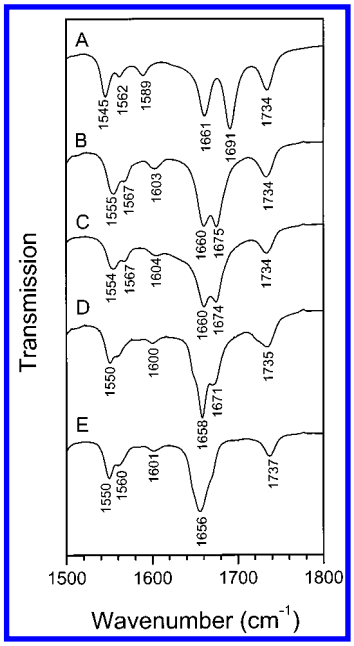

Figure 5. FT-IR spectra of (A) monomer BChl *e* in THF and aggregates of (B) R[EE]BChl *e*, (C) R[PE]BChl *e*, (D) S[PE]BChl *e*, and (E) S[IE]BChl *e* in cyclohexane. The concentrations were approximately 4 μmol mL^{-1} for all samples.

components. Chlorosomes of *Cb. phaeobacteroides* (Figure 4, panel D) show a CD spectrum with an intense type II band with a crossing point at 714 nm, slightly toward the blue side of the absorption maximum at 717 nm. The spectrum of mixed aggregates, R[EE]BChl *e* and S[IE]BChl *e* in H_2O/lecithin (1:1), shows a type II spectrum, too, but it is slightly less intense and has a zero crossing point at 709 nm.

FTIR Spectroscopy. Figure 5 shows FTIR spectra of aggregates in cyclohexane and BChl *e* monomers in THF in the region from 1500 to 1800 cm^{-1}. The frequency range from 1500 to 1630 cm^{-1} contains C═C and C═N stretching modes of the *e* macrocycle, which are sensitive to the metal coordination state.[45] Generally, B-Chls show bands at 1590−1595 and 1607−1611 cm^{-1} for six- and five-coordinated Mg, respectively.[20] The band at 1589 cm^{-1} of BChl *e* in THF indicates a six-coordinated Mg, as expected. This band shifts to 1604 and 1601 cm^{-1} in aggregates of R-BChl *e* and S-BChl *e*, respectively. The upshift of 12−15 cm^{-1} evidently reflects a change in the coordination. The frequencies of both bands are slightly lower than those observed for BChl *c* in CCl_4 but similar to those of chlorosomes. These low frequencies may reflect a relative low dielectric constant of the environment, in this case, cyclohexane.[20] Hence, as judged from the IR spectra, all four types of BChl *e* aggregates are in a five-coordinated state. It is noted that essentially all C═C and C═N stretching bands of the aggregates are clearly broader that those of the BChl *e* monomer in THF.

The bands in the 1630−1800 cm^{-1} range arise from C═O stretching vibrations. According to a previous study on Chl *b*, we assign the bands at 1661, 1691, and 1734 cm^{-1} to the C═O stretching of C-7^1 formyl, C-13^1 keto, and C-17^3 ester, respectively.[45] In aggregates of R[EE]BChl *e* and R[PE]BChl *e*, the ester band at 1734 cm^{-1} is unchanged with respect to that of BChl *e* in THF. The ester bands of aggregates of S[PE]-BChl *e* and S[IE]BChl *e* show a slight broadening and a downshift of only 3 cm^{-1}. These findings imply that the C-17^3 ester keto group is not involved in hydrogen bonding. Instead, these slight frequency shifts may reflect subtle differences in the environment of the ester group in the R-BChl and S-BChl aggregates. Despite overlapping bands of the C-7^1 formyl and C-13^1 keto bands in chlorosomes of *Cb. phaeobacteroides*, it was previously shown, using shifted excitation RR difference spectroscopy, that the C-7^1 formyl band is situated at 1660 cm^{-1} with a fwhm of 13 cm^{-1}.[22] By comparison with the formyl band of Chl *b*, the C-7^1 formyl of BChl *e* in the chlorosomes is not involved in hydrogen bonding interactions. Our IR data on BChl *e* monomers and R-BChl *e* aggregates indicate that this conclusion is also true for aggregates in cyclohexane since in both monomers and R-BChl *e* aggregates the C-7^1 formyl stretching is found at 1660 cm^{-1}. In contrast, the C-13^1 carbonyl band of R-BChl *e* aggregates is downshifted by 16 cm^{-1}, implying hydrogen bond formation. For aggregates of S[PE]-BChl *e* and S[IE]BChl *e*, the C-13^1 and C-7^1 C═O stretching region is clearly different from that of R-BChl *e* aggregates. The carbonyl region was analyzed in terms of three Lorenztian bands (data not shown) at 1651, 1660, and 1670 cm^{-1}. IR measurements in the 3000−3800 cm^{-1} region (data not shown) reveal that the C-3^1 OH is involved in hydrogen bonding in all aggregates. BChl *e* monomers exhibit sharp bands at 3503 and 3574 cm^{-1}, whereas the aggregates show broad bands with maxima at 3220−3300 cm^{-1}.

Resonance Raman Spectroscopy. As shown previously, RR spectroscopy is a sensitive tool for studying intermolecular interactions in the BChl aggregates.[10,20,23] In our case, it is a supplement to FTIR since pigment concentration and solvents are basically different. RR spectra of aggregates in aqueous media were measured in the presence of sodium dithionite to avoid photo-oxidative degradation during the measurements. The spectra in this work were obtained with 413 nm excitation, which was found to provide particularly strong resonance enhancement for the C13^1 carbonyl stretching, as compared to the 457 or 514 nm excitation.

Figure 6 shows the RR spectra in the region between 1450 and 1750 cm^{-1}. For all aggregates, the stretching modes of the *e* macrocycle are found at 1514 and 1562 cm^{-1}, in addition to a weak band at ∼1603 cm^{-1}. Chl *b* in diethyl ether showed a strong band at 1565 cm^{-1} and a weaker one at 1607 cm^{-1}, indicative of five-coordinated Mg.[45] For six-coordinated Mg, these bands would be expected at 1550−1560 and 1595 cm^{-1}. The RR spectra of the aggregates indicate that BChl *e* is exclusively in the five-coordinated state in H_2O/MGDG. In chlorosomes of *Cb. phaeobacteroides*, the corresponding coordination-state marker bands are found at 1514 (observed by 514 nm excitation; data not shown), 1560, and 1602 cm^{-1}, which reflect a five-coordinated state in the chlorosomal aggregates as well. The 1520 cm^{-1} band in the spectrum of chlorosomes is assigned to the C═C stretching mode of carotenoids.[10] For R[EE]BChl *e*, R[PE]BChl *e*, and S[PE]BChl *e*, the bands exhibit relatively large widths, analogous to our findings in the FTIR experiment. The 1562 cm^{-1} band has a fwhm of 20 cm^{-1} for these aggregates, whereas the corresponding band of S[IE]BChl *e* aggregates is substantially narrower with a fwhm of 15 cm^{-1}.

In the region above 1630 cm^{-1}, the carbonyl stretching bands of the C-13^1 carbonyl involved in aggregate formation and of the C-7^1 formyl bands are expected. In this region, the RR spectra of aggregates in H_2O/MGDG are in good agreement with the IR spectra of aggregates in cyclohexane. Aggregates of R[EE]BChl *e*, R[PE]BChl *e*, and S[PE]BChl *e* display a prominent peak at 1661 cm^{-1}, attributed to the C-7^1 formyl stretching (Figure 6). Due to the extended wings on the high- and low-frequency sides, the shape of this peak deviates from a Lorentzian (or Gaussian) line shape. A band fitting in this spectral region shows ambiguous results. In addition to the 1661

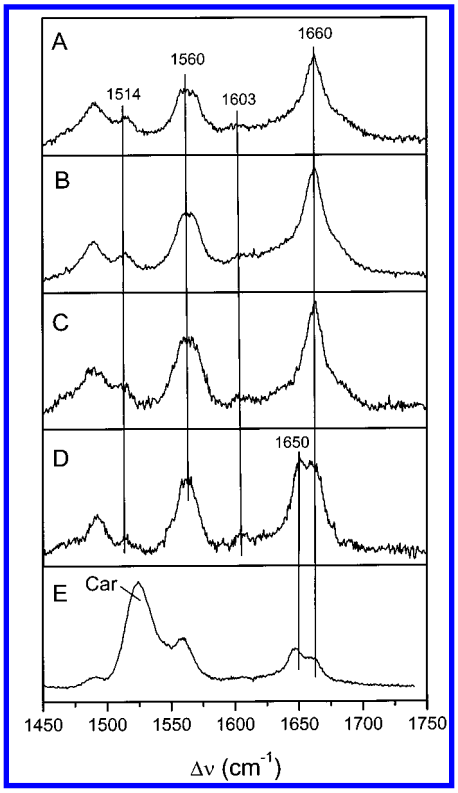

Figure 6. RR spectra of BChl *e* aggregates in H_2O/MGDG and chlorosomes of *Cb. phaeobacteroides*: (A) R[EE]BChl *e*, (B) R[PE]-BChl *e*, (C) S[PE]BChl *e*, (D) S[IE]BChl *e*, and (E) chlorosomes. Car indicates the carotenoid C═C stretching band. The excitation wavelength was 413 nm.

cm^{-1} band, four bands at 1630, 1650, 1675, and 1687 cm^{-1} (as shown in Figure 7A) or, alternatively, one very broad band centered at ca. 1660 cm^{-1} provides equally good fits. In any case, the C-13[1] C═O stretching is the only candidate; the additional bands indicate a heterogeneous environment for this carbonyl group. This heterogeneity is not present in aggregates of S[IE]BChl *e* since the wings on both sides of the C-7[1] formyl band at 1661 cm^{-1} band are replaced by a well-defined band at 1650 cm^{-1} (Figures 6D and 7F). Thus, the RR spectrum of S[IE]-BChl *e* is closely related to that of chlorosomes (cf. Figures 6E) so that 1650 cm^{-1} is readily assigned to the C-13[1] C═O stretching of the >C═O···H(X)O···Mg< structural motif of self-organized chlorosomal aggregates. Similar RR spectra were also obtained for BChl *e* aggregates in H_2O/lecithin.

We would like to point out that essentially no monomers or small oligomers are present in the aggregates of R[EE]BChl *e*, R[PE]BChl *e*, and S[PE]BChl *e*. For this reason, it is not likely that C-13[1] carbonyl is involved in hydrogen bonding with solvent molecules to any significant extent, and hence, such solvent interaction cannot explain the heterogeneity of the C═O environment. Instead, these aggregates are also characterized by the >C═O···H(X)O···Mg< structural motif, albeit with some conformational flexibility, possibly due to a less rigid overall structure of the aggregates. Consequently, the heterogeneity of the C-13[1] carbonyl environment is ascribed to different hydrogen bonding interactions, associated with the subtle variations of hydrogen bond lengths and angles of the >C═O···H(X)O···Mg< entity. Such variations are not expected to have a pronounced effect on the chlorin geometry. Indeed, in the region of the skeletal modes (1630−1450 cm^{-1}, Figure 6), the RR spectra of these aggregates reveal only a band broadening compared to S[IE]BChl *e*.

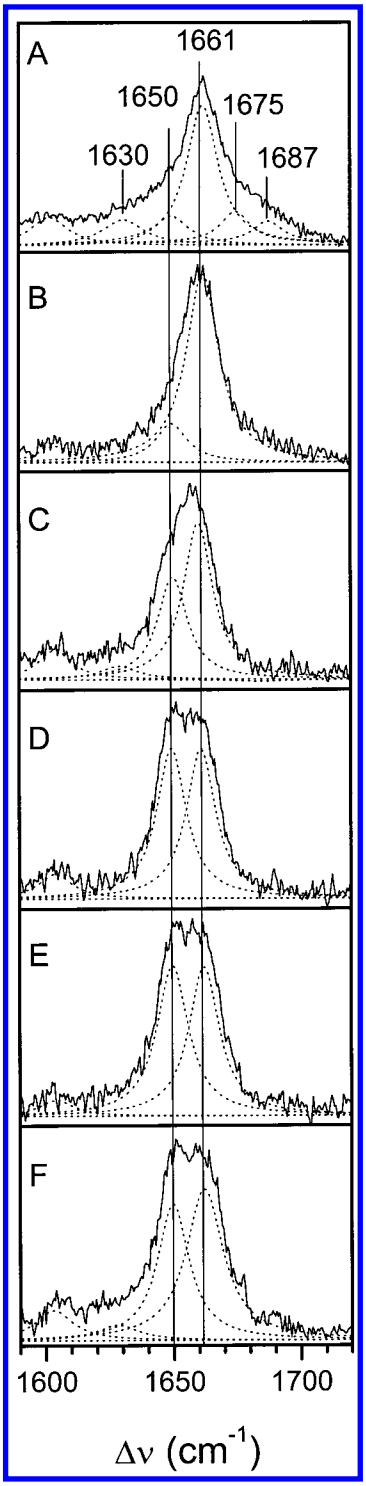

Figure 7. RR spectra of mixed aggregates of R[EE]BChl *e* and S[IE]-BChl *e* in H_2O/MGDG: (A) 100% R[EE]BChl *e*, (B) 20% S[IE]BChl *e*, (C) 40% S[IE]BChl *e*, (D) 60% S[IE]BChl *e*, (E) 80% S[IE]BChl *e*, and (F) 100% S[IE]BChl *e*. The dotted lines represent the fitted Lorentian band shapes (see text for details). The excitation wavelength was 413 nm.

To verify the results in Figure 3 (upper panel), we measured RR spectra of mixtures of R[EE]BChl *e* and S[IE]BChl *e* in H_2O/lecithin. Upon the admixture of S[IE]BChl *e* to R[EE]BChl *e*, the heterogeneity of the C-13[1] carbonyl is drastically reduced (Figure 7). Already at 20% S[IE]BChl *e*, the high-frequency wing of the 1661 cm^{-1} band has disappeared, and the only component on the low-frequency side is the 1650 cm^{-1} band. This band increases in intensity with increasing S[IE]BChl *e*

TABLE 1: Absorption, CD, IR, and RR Features of in Vitro Aggregates of BChl *e* and Chlorosomes of *Cb. phaeobacteroides*

		aggregates			
		R[EE]BChl *e*	S[IE]BChl *e*	mixed aggregate[a]	chlorosomes
abs (nm)	Q_y	706	717	717	717
CD	shape[b]	type I	type II	type II	type II
IR (cm^{-1})	C-13^1, C=O	1675	1650	1650	–
RR (cm^{-1})	C-13^1, C=O	1650, 1675, 1687	1650	1650	1646

[a] Aggregates of R[EE]BChl *e* and S[IE]BChl *e* (1:1). [b] Ref 25.

content until, at 60% S[IE]BChl *e*, the RR spectrum becomes undistinguishable from that of pure S[IE]BChl *e* aggregates. Thus, the RR data are consistent with those obtained by UV−vis absorption, IR, and CD spectroscopy and show that S[IE]-BChl *e* is essential for the formation of chlorosome-like aggregates.

4. Discussion

Our data show that BChl *e* in vitro forms basically two types of aggregates: the R[EE]BChl *e* type and the S[IE]BChl *e* type. R[PE]BChl *e* aggregates are indistinguishable from those of R[EE]BChl *e*, and S[PE]BChl *e* seems to form a precursor to the S[IE]BChl *e*-type aggregate. The characteristic spectral features of these aggregates are summarized in Table 1. It is clear that the S[IE]BChl *e*-type aggregate mimics the chlorosomal aggregates much better than do the R[EE]BChl *e*-type aggregates. Several key features for characterization of the basic aggregate interaction are evident from the data. (1) In all aggregates, Mg is found in a five-coordinated state. Moreover, there is a distinct red-shift of the aggregate Q_y absorption band relative to that of the monomer species, indicating a strong exciton interaction in a large aggregate. Consequently, the fifth magnesium ligand should be another BChl. (2) FTIR data indicate that the C-3^1 OH groups form a hydrogen bond. (3) According to FTIR and RR data, the C-13^1 carbonyl group is involved in hydrogen bond formation according to the structural motif >C=O···H(X)O···Mg<. However, in aggregates of R-BChl *e*, the C13^1 carbonyl hydrogen bond interaction is characterized by heterogeneity.

Recently, Ishii et al. studied aggregates of R[EE]BChl *c* and R[PE]BChl *c* in aqueous acetone.[46] They found that R[EE]BChl *c* and R[PE]BChl *c* formed aggregates absorbing at 714 and 730 nm, respectively. Only aggregates of R[PE]BChl *c* possessed a C=O stretching band at 1643 cm^{-1} assigned to the >C=O···H(X)O···Mg< entity. Bands at 1649 and 1657 cm^{-1} in both aggregates were assigned to C=O···Mg. The authors observed different aggregation behavior of two types of R-BChl *c*. It was suggested that these differences are significant in vivo, giving rise to different spectral pools in the chlorosomal aggregate. On one hand, these findings seem to contradict our results, which show identical aggregates of R[EE]BChl *e* and R[PE]BChl *e* aggregation. However, the polar C7^1 formyl at the BChl *e* ring might induce some significant steric hindrance that could account for the different aggregation behavior of BChl *e* species, as compared to the corresponding BChl *c* species. Another explanation might be a small but critical admixture of the S-BChl in the fraction of R[PE]BChl *c* used by Ishii et al. As we have shown in this work, such an admixture may have a significant effect on the aggregate formation (see below).

The spectral differences between the R-BChl *e* (706 nm) and S-BChl *e* (717 nm) aggregates can be interpreted in terms of different molecular organizations. Two principally different types of aggregates with the basic interaction scheme >C=O···H(X)O···Mg< can be imagined. These aggregates are based on building blocks of either closed or open dimers of BChl. In the recent NMR studies of Mizoguchi et al.[47−49] on R[EE]BChl *c* and S[IE]BChl *c* in CCl_4, the analysis of ^{13}C and ^1H aggregation shifts and ring current calculations revealed that the R-BChl species form aggregates of closed dimers whereas S-BChl aggregates consist of open dimers. It is, however, not likely that R-BChl *e* aggregates studied in this work, which show a red-shift of 60 nm with respect to the monomer species (647 nm in acetone[50]), are based on closed dimers. Closed dimes would be associated only with a modest aggregation-induced red-shift of the Q_y band.[47,48] R-BChl *c* aggregates in CCl_4 forming closed dimers displayed a Q_y band red-shift of not more than 35 nm. Thus, we conclude that in the solvents used in our work, both the R-BChl *e* and the S-BChl *e* form aggregates of open dimers.

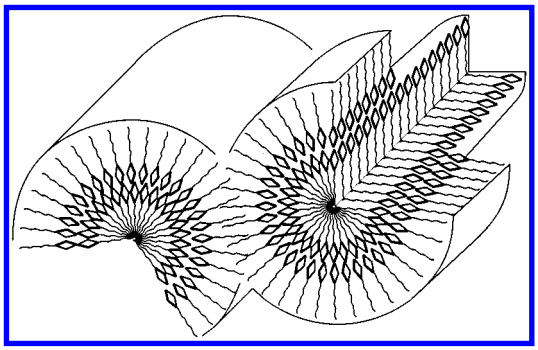

Figure 8. Cartoon models of the bilayer rod structure suggested for the BChl aggregation in *Chlorobium*. Two adjacent rods are shown. In each rod, the chlorin moieties of the inner and outer ring are located next to each other, whereas the ester side chains point in opposite directions.

A molecular modeling study showed that R[MM]BChl *d* could form a tubular aggregate with a diameter of 5 nm.[26] This study also indicated that larger substituents at C-8 and C-12 would cause a larger diameter of the tubular aggregate. This conclusion is in line with previous findings that the aggregate rod structure has a diameter of 10 nm in chlorosomes of *Chlorobium*.[19] Solid-state NMR has indicated that two different interstack interactions are present in the chlorosomes of *Chlorobium tepidum*.[27] Moreover, solution NMR spectroscopy of S[IE]BChl *e* in CCl_4 demonstrated that the BChl stacks formed by the coordination of adjacent BChls may exist in both anti and syn configurations with anti and syn designating the orientation of the fifth ligand of magnesium with respect to the orientation of the C-17−C-17^1 bond.[47]

We interpret the these findings in terms of a supramolecular aggregate forming a bilayer in which all interactions are based on the scheme >C=O···H(X)O···Mg< of open dimers but such that the curvature in the two layers are opposite each other, i.e., in the outer layer the esterifying alcohols at C-17 are directed toward the outside whereas in the inner layer these side chains are directed toward the center of the rod. The outer ring would have the structure proposed by Holzwarth and Schaffner.[26] A sketch of this refined model is shown in Figure 8. This model for the chlorosome aggregate structure is supported by a recent heteronuclear CP-MAS NMR study on chlorosomes from *Cb.*

tepidum.[51] The model described above is strongly supported and invoked by a recent study on the solid BChl *a* aggregate, where a similar bilayer sheet structure was proposed.[52] The bilayer rod model implies that two networks of aggregating chlorin rings are close together. We propose that only when this bilayer structure is formed are the strong red-shifted chlorosome-like spectral features observed. Applying this model to our results suggests that R-BChl *e* in vitro favors aggregates in which the ester chains are directed outward, whereas S-BChl *e* may form tubular structures with both curvatures, which therefore give rise to the chlorosome-like spectral features. In aggregates of mixed R-BChl *e* and S-BChl *e*, as is the case in chlorosomes, R-BChl *e* would preferentially form the outer ring only, whereas S-BChl *e* predominantly would form the inner ring of the bilayer. This model, which remains to be tested experimentally, would also provide an answer to the long-standing question of what "fills the hole" in a chlorosome rod. It could be a second BChl rod aggregate with the ester chains directed toward the center of the rod.

In this report, we have also provided an answer to the question raised by Olson and Cox[53] of why only S-BChl stereoisomers form chlorosome-like aggregates when most chlorosomal BChls are found as R-BChl? We were able to show that the addition of small amounts of S-BChl *e* causes the reorganization of the R[EE]BChl *e*-type aggregate absorbing at 706 nm to a chlorosome-like aggregate absorbing at 717 nm. This conclusion is in line with our recent data indicating that BChl *c* aggregate formation is an autocatalytic process.[39] Recently, it was noted that the choice of the nonpolar solvent for the formation of aggregates as chlorosome models should be made with care to obtain good models.[54] We have shown in this work that the stereochemistry of the BChl species is a crucial parameter for mimicking the chlorosomal aggregate structure.

Acknowledgment. The authors acknowledge the technical assistance of M. Trinoga. This work was supported by a TMR project on "Green bacterial photosynthesis", Grant FM RX-CT960081, by the European Commission. Dr. M. Miller, University of Southern Denmark in Odense, kindly provided the chlorosomes of *Cb. phaeobacteroides*.

References and Notes

(1) Blankenship, R. E.; Olson, J. M.; Miller, M. In *Anoxygenic Photosynthetic Bacteria*; Blankenship, R. E., Madigan, M. T., Bauer, C. E., Eds.; Kluwer Academic Publishers: Dordrecht, The Netherlands, 1995; pp 399−435.

(2) Olson, J. M. *Photochem. Photobiol.* **1998**, *67*, 61−75.

(3) Matthews, B. W.; Fenna, R. E.; Bolognesi, M.; Schmid, M. F.; Olson, J. M. *J. Mol. Biol.* **1979**, *131*, 259−258.

(4) Kühlbrandt, W.; Wang, D. N.; Fujiyoshi, Y. *Nature* **1994**, *367*, 614−621.

(5) Sidler, W. A. In *The Molecular Biology of Cyanobacteria*; Bryant, D. A., Ed.; Kluwer Academic Publishers: Dordrecht, The Netherlands, 1994; pp 139−216.

(6) Bystrova, M. I.; Mal'gosheva, I. N.; Krasnovskii, A. A. *Mol. Biol. (Moscow)* **1979**, *13*, 440−451.

(7) Smith, K. M.; Kehres, L. A.; Fajer, J. *J. Am. Chem. Soc.* **1983**, *105*, 1387−1389.

(8) Griebenow, K.; Holzwarth, A. R. *Biochim. Biophys. Acta* **1989**, *973*, 235−240.

(9) Balaban, T. S.; Holzwarth, A. R.; Schaffner, K.; Boender, G. J.; de Groot, H. J. M. *Biochemistry* **1995**, *34*, 15259−15266.

(10) Hildebrandt, P.; Griebenow, K.; Holzwarth, A. R.; Schaffner, K. *Z. Naturforsch.* **1991**, *46C*, 228−232.

(11) Miller, M.; Gillbro, T.; Olson, J. M. *Photochem. Photobiol.* **1993**, *57*, 98−102.

(12) Gerola, P. D.; Olson, J. M. *Biochim. Biophys. Acta* **1986**, *848*, 69−76.

(13) Sakuragi, Y.; Frigaard, N.-U.; Shimada, K.; Matsuura, K. *Biochim. Biophys. Acta* **1999**, *1413*, 172−180.

(14) Schmidt, K. *Arch. Microbiol.* **1980**, *124*, 21−31.

(15) Frigaard, N.-U.; Takaichi, S.; Hirota, M.; Shimada, K.; Matsuura, K. *Arch. Microbiol.* **1997**, *167*, 343−349.

(16) Bobe, F. W.; Pfennig, N.; Swanson, K. L.; Smith, K. M. *Biochemistry* **1990**, *29*, 4340−4348.

(17) Borrego, C. M.; Gerola, P. D.; Miller, M.; Cox, R. P. *Photosynth. Res.* **1999**, *59*, 159−166.

(18) Staehelin, L. A.; Golecki, J. R.; Fuller, R. C.; Drews, G. *Arch. Microbiol.* **1978**, *119*, 269−277.

(19) Staehelin, L. A.; Golecki, J. R.; Drews, G. *Biochim. Biophys. Acta* **1980**, *589*, 30−45.

(20) Lutz, M.; Van Brakel, G. In *Green Photosynthetic Bacteria*; Olson, J. M., Ormerod, J. G., Amesz, J., Stackebrandt, E., Trüper, H. G., Eds.; Plenum Press: New York, 1988; pp 23−34.

(21) Brune, D. C.; King, G. H.; Blankenship, R. E. In *Photosynthetic Light-Harvesting Systems*; Scheer, H., Schneider, S., Eds.; de Gruyter: Berlin, 1988; pp 141−151.

(22) Feiler, U.; Albouy, D.; Lutz, M.; Robert, B. *Photosynth. Res.* **1994**, *41*, 175−180.

(23) Hildebrandt, P.; Tamiaki, H.; Holzwarth, A. R.; Schaffner, K. *J. Phys. Chem.* **1994**, *98*, 2192−2197.

(24) Betti, J. A.; Blankenship, R. E.; Natarajan, L. V.; Dickinson, L. C.; Fuller, R. C. *Biochim. Biophys. Acta* **1982**, *680*, 194−201.

(25) Griebenow, K.; Holzwarth, A. R.; van Mourik, F.; van Grondelle, R. *Biochim. Biophys. Acta* **1991**, *1058*, 194−202.

(26) Holzwarth, A. R.; Schaffner, K. *Photosynth. Res.* **1994**, *41*, 225−233.

(27) van Rossum, B.-J.; Boender, G. J.; Mulder, F. M.; Raap, J.; Balaban, T. S.; Holzwarth, A. R.; Schaffner, K.; Prytulla, S.; Oschkinat, H.; de Groot, J. J. M. *Spectrochim. Acta A* **1998**, *54*, 1167−1176.

(28) Hirota, M.; Moriyama, T.; Shimada, K.; Miller, M.; Olson, J. M.; Matsuura, K. *Biochim. Biophys. Acta* **1992**, *1099*, 271−274.

(29) Uehara, K.; Mimuro, M.; Ozaki, Y.; Olson, J. M. *Photosynth. Res.* **1994**, *41*, 235−243.

(30) Miyatake, T.; Tamiaki, H.; Holzwarth, A. R.; Schaffner, K. *Helv. Chim. Acta* **1999**, *82*, 797−810.

(31) van Noort, P. I.; Zhu, Y.; Lobrutto, R.; Blankenship, R. E. *Biophys. J.* **1997**, *72*, 316−325.

(32) Olson, J. M.; Pedersen, J. P. *Photosynth. Res.* **1990**, *25*, 25−37.

(33) Balaban, T. S.; Holzwarth, A. R.; Schaffner, K. *J. Mol. Struct.* **1995**, *349*, 183−186.

(34) Balaban, T. S.; Tamiaki, H.; Holzwarth, A. R.; Schaffner, K. *J. Phys. Chem. B* **1997**, *101*, 3424−3431.

(35) Chiefari, J.; Griebenow, K.; Fages, F.; Griebenow, N.; Balaban, T. S.; Holzwarth, A. R.; Schaffner, K. *J. Phys. Chem.* **1995**, *99*, 1357−1365.

(36) Wahlund, T. M.; Woese, C. R.; Castenholz, R. W.; Madigan, M. T. *Arch. Microbiol.* **1991**, *156*, 81−90.

(37) van Walree, C. A.; Sakuragi, Y.; Steensgaard, D. B.; Bösinger, C. S.; Frigaard, N.-U.; Cox, R. P.; Holzwarth, A. R.; Miller, M. *Photochem. Photobiol.* **1999**, *69* (3), 322−328.

(38) Steensgaard, D. B.; Cox, P. R.; Miller, M. *Photosynth. Res.* **1996**, *48*, 385−393.

(39) Balaban, T. S.; Leitich, J.; Holzwarth, A. R.; Schaffner, K. *J. Phys. Chem. B* **2000**, *104*, 1362−1372.

(40) Borrego, C. M.; Arellano, J. B.; Abella, C. A.; Gillbro, T.; Garcia-Gil, J. *Photosynth. Res.* **1999**, *60*, 257−264.

(41) Wackerbarth, H.; Klar, U.; Günther, W.; Hildebrandt, P. *Appl. Spectrosc.* **1999**, *53*, 283−291.

(42) Smith, K. M.; Simpson, D. J. *J. Chem. Soc., Chem. Commun.* **1986**, *777*, 1682−1684.

(43) Alden, R. G.; Lin, S. H.; Blankenship, R. E. *J. Lumin.* **1992**, *51*, 51−66.

(44) Keller, D.; Bustamante, C. *J. Chem. Phys.* **1986**, *84*, 2972−2980.

(45) Tasumi, M.; Fujiwara, M. *Adv. Spectrosc.* **1987**, *14*, 407−428.

(46) Ishii, T.; Uehara, K.; Ozaki, Y.; Mimuro, M. *Photochem. Photobiol.* **1999**, *750*, 765.

(47) Mizoguchi, T.; Sakamoto, S.; Koyama, Y.; Ogura, K.; Inagaki, F. *Photochem. Photobiol.* **1998**, *67*, 239−248.

(48) Mizoguchi, T.; Ogura, K.; Inagaki, F.; Koyama, Y. *Biospectroscopy* **1999**, *5*, 63−77.

(49) Mizoguchi, T.; Limantara, L.; Matsuura, K.; Shimada, K.; Koyama, Y. *J. Mol. Struct.* **1996**, *379*, 249−265.

(50) Scheer, H. In *Chlorophylls*; Scheer, H., Ed.; CRC Press: Boca Raton, FL, 1991; pp 3−30.

(51) van Rossum, B.-J.; Steensgaard, D. B.; Mulder, F. M.; Boender, G. J.; Schaffner, K.; Holzwarth, A. R.; de Groot, H. J. M. *Biochemistry*, submitted for publication.

(52) van Rossum, B.-J.; Schulten, E. A. M.; Oschkinat, H.; de Groot, H. J. M. *J. Am. Chem. Soc.*, submitted for publication.

(53) Olson, J. M.; Cox, R. P. *Photosynth. Res.* **1991**, *30*, 35−43.

(54) Umetsu, M.; Wang, Z. Y.; Zhang, J.; Ishii, T.; Uehara, K.; Inoko, Y.; Kobayashi, M.; Nozawa, T. *Photosynth. Res.* **1999**, *60*, 229−239.